

Recharging scenarios for differently electrified road vehicles: A methodology and its application to the Italian grid

Original

Recharging scenarios for differently electrified road vehicles: A methodology and its application to the Italian grid / Gerboni, R., Caballini, C., Minetti, A., Grosso, D., Dalla Chiara, B.. - In: TRANSPORTATION RESEARCH INTERDISCIPLINARY PERSPECTIVES. - ISSN 2590-1982. - 11:(2021), p. 100454. [10.1016/j.trip.2021.100454]

Availability:

This version is available at: 11583/2921477 since: 2021-09-06T13:21:53Z

Publisher:

Elsevier

Published

DOI:10.1016/j.trip.2021.100454

Terms of use:

This article is made available under terms and conditions as specified in the corresponding bibliographic description in the repository

Publisher copyright

Elsevier postprint/Author's Accepted Manuscript

© 2021. This manuscript version is made available under the CC-BY-NC-ND 4.0 license
<http://creativecommons.org/licenses/by-nc-nd/4.0/>. The final authenticated version is available online at:
<http://dx.doi.org/10.1016/j.trip.2021.100454>

(Article begins on next page)

PAPER REF: 20071

ACTIVE THERMOGRAPHY TECHNIQUE FOR FATIGUE DAMAGE CHARACTERIZATION IN GEARS

Francesca Curà, Raffaella Sesana, Luca Corsaro^(*)

DIMEAS, Department of Mechanical and Aerospace engineering, Polytechnic of Torino, Torino, Italy

(*)Email: luca.corsaro@polito.it

ABSTRACT

Active Thermography (AT) is a Non Destructive Technique (NDT) that may be an efficient alternative to evaluate possible microstructural alterations inside materials due to damaging conditions. In this paper, a fatigue damage identification on two different gears (*standard* and *thin-rim*) was conducted by using an AT approach with a Lock-In technique. Both gears were previously tested under bending fatigue conditions, by loading the teeth at the so called Single Contact Point by a dedicated equipment. Damaged and undamaged zones were identified, phase maps and thermal diffusivities were estimated. In this way, a possible fatigue damage characterisation was pointed out by using the thermal diffusivity variation as damage parameter.

Keywords: standard gear, light weight gear, fatigue, Active Thermography, Lock-In analysis, phase map, thermal diffusivity.

INTRODUCTION

Microstructural alterations and plasticisation may represent the classical effects of fatigue damage in materials and components. These effects are generally related to working conditions (as applied load or number of cycles).

In gears, a classical fatigue condition consists in a continuous tooth bending due to meshing and, in some cases, a failure at the tooth root zone occurs. This phenomenon was widely discussed by many authors, focusing as an example on the gear's geometry that may affect both nucleation and propagation crack path during bending fatigue conditions [1][2][3]. From the experimental point of view, Non Destructive Techniques (NDT) as Digital Image Correlation (DIC) and Passive Thermography (PT) were adopted to investigate both tooth root stress field and most stressed point position in gears with different geometries (standard and light weight gears) ([4], [5]), highlighting safe and catastrophic crack propagation paths during bending fatigue tests. In particular, the tested gears showed a different thermal behaviour and in particular the light weight gear exhibited a strong heat dissipation flow due to the high displacements involved in fatigue tests. These results draw the attention to how the gear's geometry can be differently involved during the operating conditions.

Over the years, PT was widely used to characterise the fatigue damage in materials and components. More recently, Thermography in Active configuration (Active Thermography, AT), also called "stimulated thermography", became attractive to detect hidden defects, and the scientific literature is full of papers describing methods and algorithms to improve defects visibility [6][7][8][9][10].

In case of materials characterization, an Active Thermography setup was recently successfully developed to estimate thermal diffusivity values of thermal barrier coatings (TBCs) [11][12]

and Aerogel materials [13], according to ISO 18555 and ISO 18755 Standards. To that aim, both pulsed and Lock-In configurations were adopted.

Fatigue damage phenomena were also studied by using Active Thermography techniques in [14][15], where some algorithms related to phase map results were utilised to evaluate both crack growth and possible crack tip locations. In [16] Passive and Active approaches were adopted to characterise specimens subjected to High Cycle tests, in order to relate the thermal diffusivity variation of each sample to the corresponding variation of traditional parameters as surface thermal increment and hysteresis loop area. In particular, an Active Thermography in Lock-In configuration was chosen for diffusivity measurements [17].

In this work, the thermal diffusivity was considered as fatigue damage index for *standard* and *thin-rim* gears subjected to bending cycles. In particular, damaged and undamaged zones of gears were thermally excited in Lock-In configuration with the aim to evaluate the effect of microstructural alterations basing on thermal data processing.

MATERIALS AND METHODS

Two types of spur gears (one *standard* and one *thin-rim* gears) were considered in this work. Geometrical parameters of the two tested gears are resumed in Table 1. In particular are shown: pitch diameter (dp), face width (b), number of teeth (z), modulus (m), backup ratio (rim dimension respect to the tooth height) (mb), web ratio (web thickness respect to the face width) (mw) and gear blank factor (CR) [18]. Each gear is made of C45 steel without thermal treatments. Technical drawings of both the tested gears (*standard* and *thin-rim*) are shown in Figure 1.

Table 1 – Gears geometry.

	dp [mm]	b [mm]	z	m [mm]	mb	mw	CR
Standard	96	20	32	3	1	1	1
Thin-rim	96	20	32	3	0,5	0,1	0.59

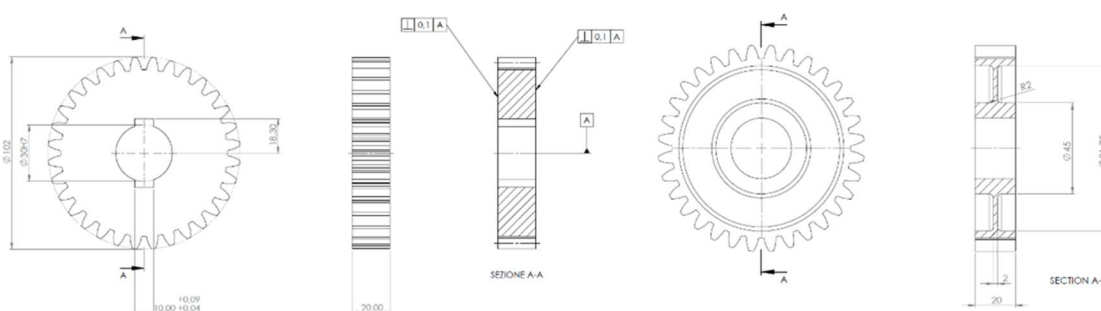


Fig. 1 – Technical drawings of *standard* (left side) and *thin-rim* (right side) gear.

Gears (*standard* and *thin-rim*) were previously tested under bending fatigue conditions, by loading the teeth at the so called Single Contact Point [19] with a dedicated device [5].

The experimental equipment for damage characterisation is an Active Thermography (AT) setup, shown in Figure 2 (left side). It is composed of a IR thermo camera, a laser excitation source and a PC control unit. The IR thermo camera is a FLIR A6751sc with sensitivity lower than 20 mK and 3-5 μm spectral range, while the laser source can generate a maximum power

of 50 W concentrated in a small surface. The “reflection mode” configuration was adopted and gears were located 400 mm distance from the thermal camera. The frame rate acquisition was 785.67 Hz.

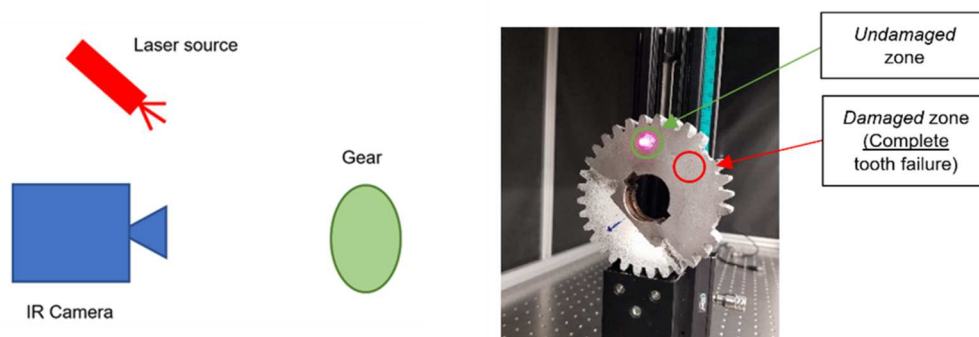


Fig. 2 – Experimental setup scheme (left side) and *standard* gear under test (right side).

Three zones (undamaged, ND, and damaged, D1, D2) for *standard* gear and four zones (undamaged, ND, and damaged, D1, D2, D3) for *thin-rim* gear were tested with the Lock-In technique (as an example, see Figure 2 (right side) for *standard* gear).

More in detail, the damaged zones (D) are located close to the tooth failure occurred during the bending fatigue test, while the undamaged (ND) zones correspond to areas under untested teeth and they are located far from the damaged (D) areas. Undamaged, ND, and damaged, D, zones concern both tested gears (*standard* and *thin-rim*); damaged (D) zones involve cases characterised by complete tooth failures (where the tooth was completely removed) or simply by crack initiations at the tooth root.

Lock-In Active Thermography technique was adopted in this activity. A periodic heating was generated on the component surface and amplitude or phase images are here used as results. Each zone (undamaged, ND, and damaged, D) was thermally excited by using 20 replications of a square wave (duty cycle equal to 50%) with a time period of 2000 ms and a power of 25 W. The corresponding phase images of each test were then processed by using IRTA2 Software, and phase profiles were extracted from a horizontal line at the first Lock-In frequency (0.5 Hz). Lines are located in the centre of the phase maps, as illustrated in Figure 3.

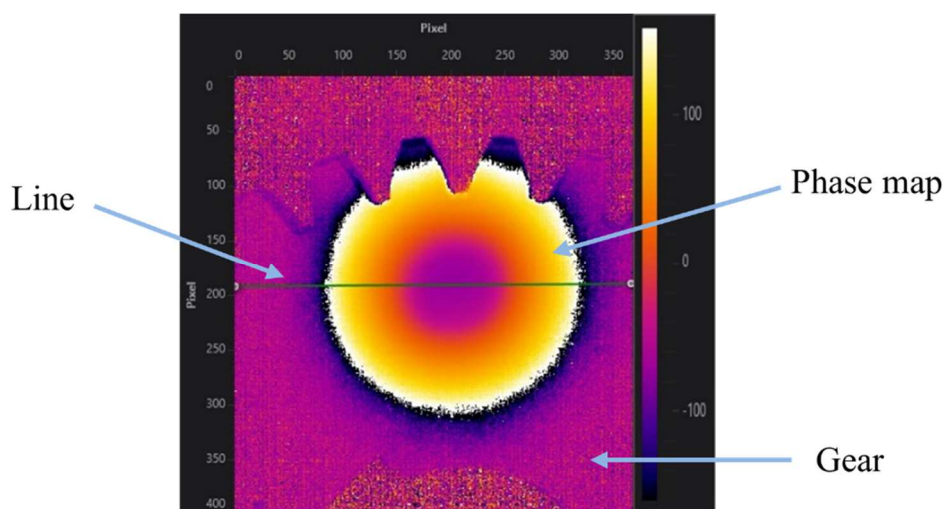


Fig. 3 – *Standard* gear phase map and the line location.

A thermal diffusivity estimation was performed starting from the phase profiles. More in detail, Equation (1) shows how to compute the thermal diffusivity, as depicted in [17].

$$m = \sqrt{\pi f / \alpha} \quad (1)$$

The thermal diffusivity, α , is a function of the phase profile slope, m , and the Lock-In frequency, f (Hz). Phase profiles in radiant unit and pixel-to-mm conversion factors are required. Moreover, a rephasing signal was necessary to generate the phase profile with a continuous slope. This way, phase profiles and the corresponding thermal diffusivities variations may represent a possible fatigue damage index.

RESULTS AND CONCLUSIONS

Experimental results for both tested gears (*standard* and *thin-rim*) are presented in this section. An example of *standard* gear phase map is shown in Figure 4 (undamaged zone, ND, on the left side and damaged zone, D1, on the right side). A complete tooth failure is clearly visible on the right phase map of Figure 4 (D1 zone).

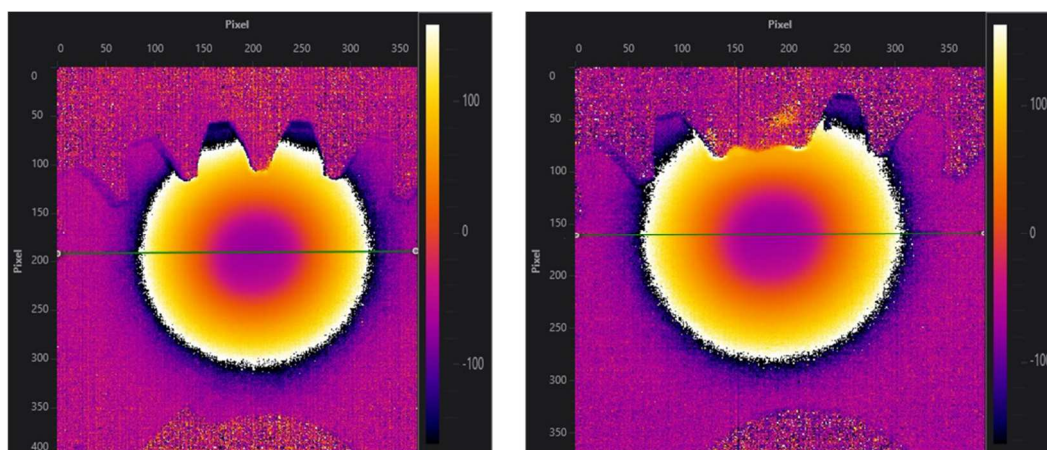


Fig. 4 – *Standard* gear phase map (undamaged zone, ND, left side - damaged zone, D1, right side).

Phase profiles were extracted from the phase maps of each test. Figure 5 compares *standard* gear phase profiles extracted respectively from undamaged (ND) and damaged (D) zones (D1 and D2 zones refer to complete tooth failures). One replication is illustrated, and profiles were plotted in a limited pixel range to emphasize the slopes between undamaged (ND) and damaged (D) zones.

Similar results are shown in Figures 6 and 7 for the *thin-rim* gear. In particular, Figure 6 shows an example of *thin-rim* gear phase maps, while the corresponding *thin-rim* gear phase profiles are illustrated in Figure 7. Both results refer to undamaged (ND) and damaged (D) zones. More in detail, D3 test refers to an incomplete tooth failure where the crack propagation just started, while D1 and D2 refer to cases where teeth were completely removed.

Thermal diffusivities computations are illustrated in Table 2 and results are referred to a mean value of three experimental tests. More in detail, it resumes: phase profile slope (m), R-square value corresponding the phase profile approximation (R^2) and thermal diffusivity (α in [m^2/s]) computed with Equation (1).

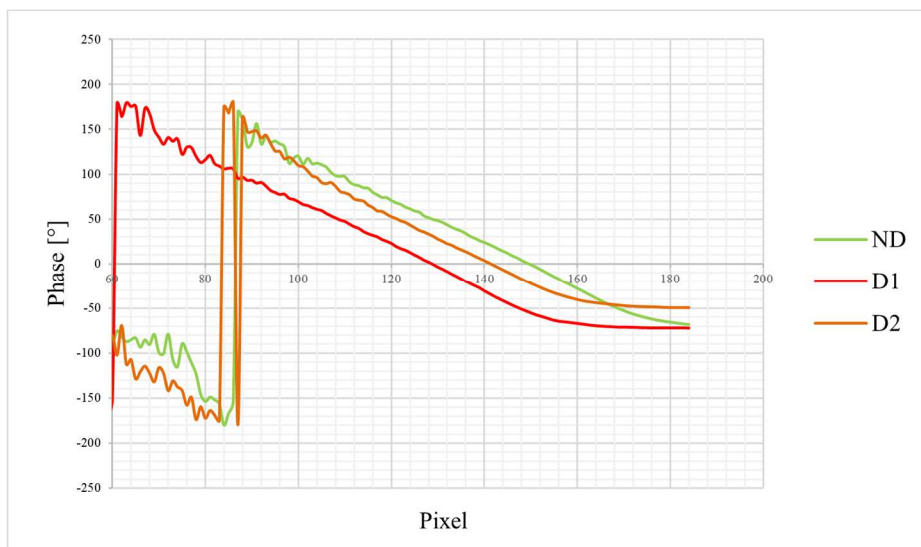


Fig. 5 – Standard gear phase profiles.

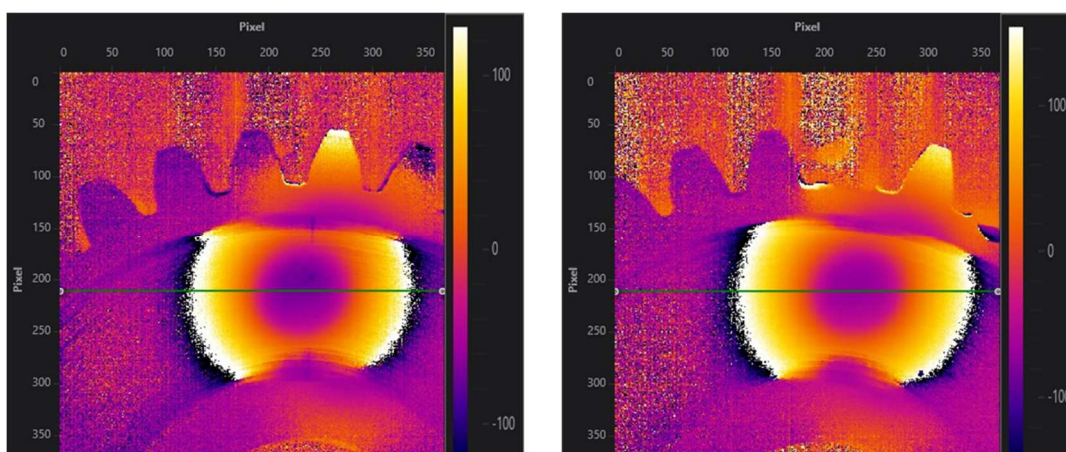


Fig. 6 – Thin-rim gear phase map (undamaged zone, ND, left side - damaged zone, D1, right side).

Table 2 – Thermal diffusivities results.

	Standard gear			Thin-rim gear		
	m	R^2	α	m	R^2	α
ND	0.0426	0.99	8.84E-06	0.0472	0.99	7.23E-06
D1	0.0437	0.99	8.44E-06	0.0507	0.99	6.28E-06
D2	0.0443	0.99	8.19E-06	0.0524	0.99	5.86E-06
D3	-	-	-	0.0515	0.99	6.07E-06

Figure 8 compares the thermal diffusivity variation between undamaged (ND) and damaged (D) zones. A mean value was computed for the damaged (D) zones of each tested gear (*standard* and *thin-rim*).

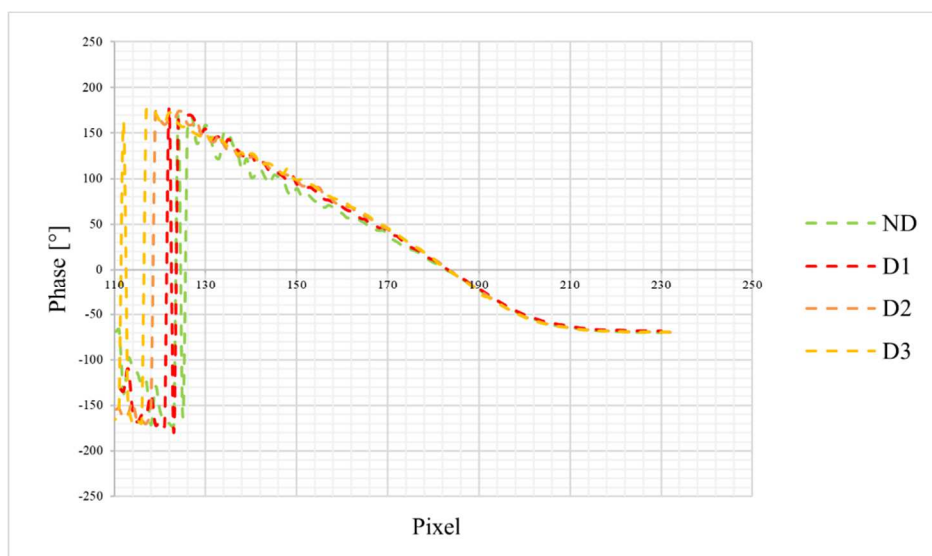


Fig. 7 – Thin-rim gear phase profiles.

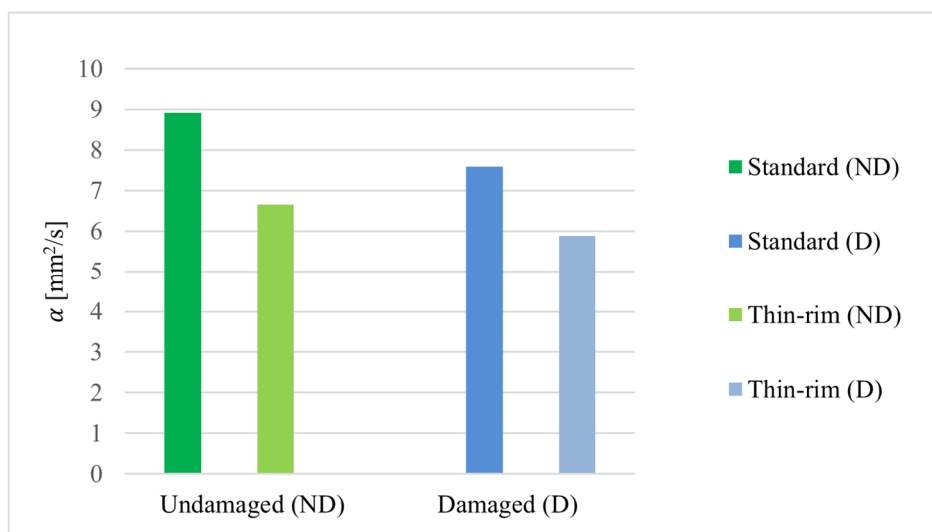


Fig. 8 – Thermal diffusivities comparison for *standard* and *thin-rim* gears.

From the analysis of results, the thermal diffusivity variation may represent a fatigue damage index for *standard* and *thin-rim* gears subjected to bending fatigue. A thermal diffusivity reduction is pointed out between the undamaged (ND) and damaged (D) zones on the basis of microstructural alterations due to the fatigue damage. A different thermal diffusivity value was also obtained for the undamaged (ND) zones of both the gears (*standard* and *thin-rim*). Gears were manufactured with the same material (see Material and methods section), but with different production process. As a matter of fact, geometries of tested gears change substantially in the part under the teeth for both backup and web ratio (see Table 1 and Figure 1). As a consequence of that, web and rim parts of *thin-rim* gear requires different machining process with respect to a classical *standard* gear. As well known, machining process introduces microstructural alterations as residual stresses and, as expected, a thermal diffusivity variation between the undamaged (ND) zones is highlighted.

CONCLUSIONS

The results obtained in the present work allow to draw the following conclusions:

Both gears (*standard* and *thin-rim*) were tested under bending fatigue conditions up to a tooth failure occurs. D3 Damaged zone considers an incomplete tooth failure with a crack propagation at the tooth root zone. In this way, the effect of an incomplete tooth failure on thermal diffusivities was evaluated and the result was according to those obtained for a complete tooth failure. In any case, to overcome this impasse, thermal diffusivity was always computed along the horizontal direction.

Undamaged (ND) and damaged (D) zones show the same surface aspect. As a consequence of that, thermal diffusivity variations may be only related to possible microstructure alterations as results of the fatigue damage. As a matter of fact, the effect of tooth bending tests on the central part of gears, in particular on the web geometry (for *thin-rim* gear), was already observed during the Passive Thermography approach.

Lock-In technique potentiality allows to estimate the thermal diffusivity values in a very fast and easy way. A dedicated tuning on the setup parameter is necessary to achieve the best phase profiles slope.

Finally, the thermal diffusivity variation may be satisfactory used as damage index also in complex components as *standard* and *thin-rim* gears.

REFERENCES

- [1] Lewicki DG, Crack propagation studies to determine benign or catastrophic failure modes for aerospace thin-rim gears. NASA Technical Memorandum 107170, 1996.
- [2] Lewicki DG, Ballarini R, Rim thickness effects on gear crack propagation life. Int. J. Fracture, 1997, 87 pp.59-86.
- [3] Curà F, Mura A, Rosso C, Effect of rim and web interaction on crack propagation paths in gears by means of XFEM technique. Fatigue Fract Eng Mater Struct, 2015, 38/10, pp.1237-1245.
- [4] Curà F, Mura A, Corsaro L, Revilla A, DIC analysis of gears in bending condition. IOP Conf. Series: Materials Science and Engineering, 2023, 1275 012038, DOI 10.1088/1757-899X/1275/1/012038.
- [5] Curà F, Mura A, Corsaro L, Experimental investigation on crack propagation paths in spur gears. IOP Conf. Series: Materials Science and Engineering, 2022, 1214 12029, DOI 10.1088/1757-899X/1214/1/012029.
- [6] He Y, Tian G, Pan M, Chen D, Eddy current pulsed phase thermography and feature extraction. Applied physics letters, Aug. 2013, 103:8, pp.084104, doi: 10.1063/1.4819475.
- [7] Ben Larbi W, Klein M, Bendada A, Maldague X, Experimental Comparison of Lock-in and Pulsed Thermography for the Nondestructive Evaluation of Aerospace Materials. 6th International Workshop, Advances in Signal Processing for Non Destructive Evaluation of Materials (IWASPNDE), 2009, Ontario, Canada.
- [8] Liu J, Yang W, Dai J, Research on thermal wave processing of lock-in thermography based on analyzing image sequences for NDT. Infrared physics and technology, Sep. 2010, 53:5, pp.348-357, doi: 10.1016/j.infrared.2010.06.002.

- [9] Ibarra-Castanedo C, Piau JM, Guilbert S, Avdelidis NP, Genest M, Bendada A, Maldague X, Comparative Study of Active Thermography Techniques for the Nondestructive Evaluation of Honeycomb Structures. *Research in Nondestructive Evaluation*, 2009, 20:1, pp.1-31, DOI: 10.1080/09349840802366617
- [10] Halloua H, Obbadi A, Errami Y, Sahnoun S, Elhassnaoui A, Nondestructive inverse approach for determining thermal and geometrical properties of internal defects in CFRP composites by lock-in thermography. *Proc. Int. Conf. Electr. Sci. Technol. Maghreb, Cist.* 2016, pp.1-7, doi: 10.1109/CISTEM.2016.8066828.
- [11] Curà F, Sesana R, Corsaro L, Mantoan R, Active thermography technique for barrier coatings characterization. *IOP Conf. Series: Materials Science and Engineering*, 2022, 1214 012034, DOI 10.1088/1757-899X/1214/1/012034.
- [12] Curà F, Sesana R, Corsaro L, Mantoan R, Characterization of Thermal Barrier Coatings Using an Active Thermography Approach. *Ceramics 5.4*, 2022, pp.848-61, <https://doi.org/10.3390/ceramics5040062>.
- [13] Curà F, Sesana R, Dugand M, Corsaro L, Active thermography characterization of aerogel materials for vehicle electrification. *IOP Conf. Series: Materials Science and Engineering*, 2023, 1275 012014, DOI 10.1088/1757-899X/1275/1/012014.
- [14] An YK, Min Kim J, Sohn H, Laser lock-in thermography for detection of surface-breaking fatigue cracks on uncoated steel structures. *NDT E Int.*, Jul. 2014, 65, pp.54-63, doi: 10.1016/j.ndteint.2014.03.004.
- [15] Hwang S, An Y, Kim J, Sohn H, Monitoring and Instantaneous Evaluation of Fatigue Crack Using Integrated Passive and Active Laser Thermography. *Optics and Lasers in Engineering*, 2019, 119, pp.9-17. Web.
- [16] Curà F, Sesana R, Corsaro L, Santoro L, La termografia attiva applicata allo studio della fatica nei materiali metallici: un caso studio. *AIPnD 2022 - Conferenza Nazionale sulle Prove Non Distruttive, Monitoraggio e Diagnostica*, Verona 19-21 October 2022.
- [17] Mendioroz A, Fuente-Dacal R, Apiñaniz E, Salazar A, Thermal Diffusivity Measurements of Thin Plates and Filaments Using Lock-in Thermography. *Review of Scientific Instruments*, 2009, 80:7, pp.074904.
- [18] Standard ISO 6336, Calculation of Load Capacity of Spur and Helical Gears, Part 1, International Standard Organization, 2019.
- [19] Standard ISO 6336, Calculation of Load Capacity of Spur and Helical Gears, Part 3, International Standard Organization, 2019.